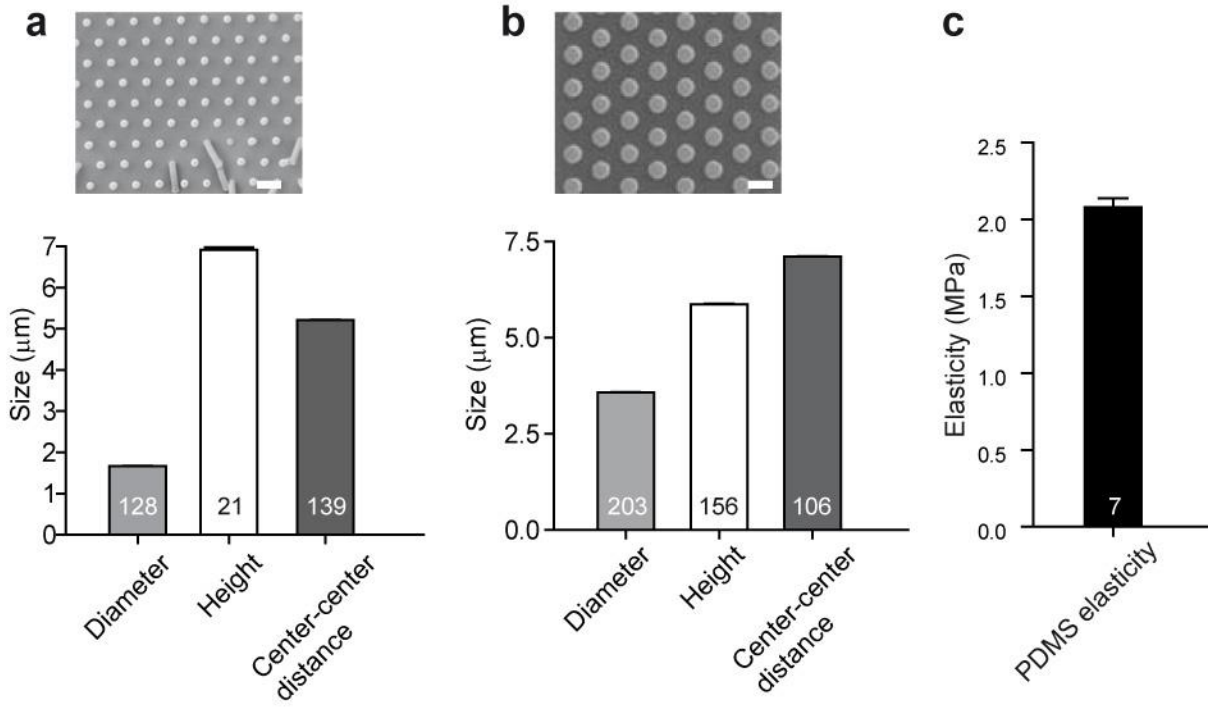

Supplementary Figure 1: Physical properties of pillar arrays

(**a,b**) Dimensions of individual pillar elements determined from scanning electron micrographs (SEM). SEM images (scale bar 5 µm) were acquired from either square or side-on of pillar arrays sputtered with gold. The diameter and center-center distance were determined from images taken square to the array and the height was calculated from images taken perpendicular to the individual elements. In all cases 5 individual masters were used to cast arrays for imaging and multiple elements from each were measured, offline, using ImageJ. Data are displayed as mean ± s.e.m.; *n* indicates number of individual elements measured. (**c**) Blocks of PDMS cured under the same conditions as the pillar arrays were probed using atomic force spectroscopy to determine PDMS elasticity. At least 250 force-distance curves were obtained on each of 7 PDMS samples, in PBS using a silicon cantilever with a spring constant of 0.125 N/m. Elasticity was calculated using the Hertz model for measurements made with a pyramidal indentor.

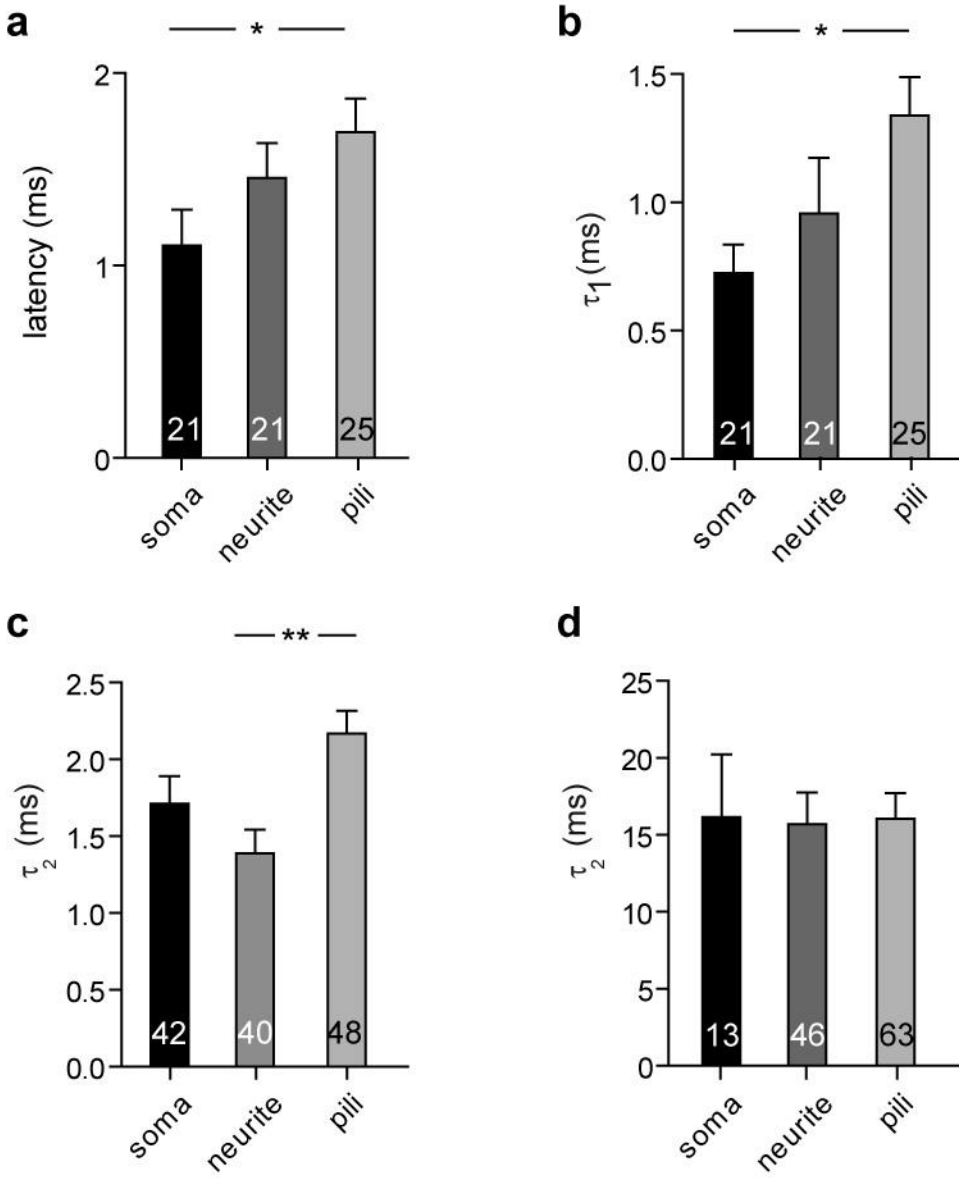

Supplementary Figure 2: Current kinetics as measured using different methods.

In order to compare current latencies (**a**) and the activation time constant (τ_1, **b**) values were averaged for each cell and then an average of these values was taken. Data displayed as mean ± s.e.m. and *n* indicates number of cells. Soma and neurite indentation measurements were matched, i.e. taken from the same cell. In order to compare the inactivation time constant (τ_2, **c** (RA-currents), **d** (IA-currents)) each individual current was used as a data point due to the variability in each individual cell, as such *n* indicates number of currents measured, data is mean ± s.e.m.

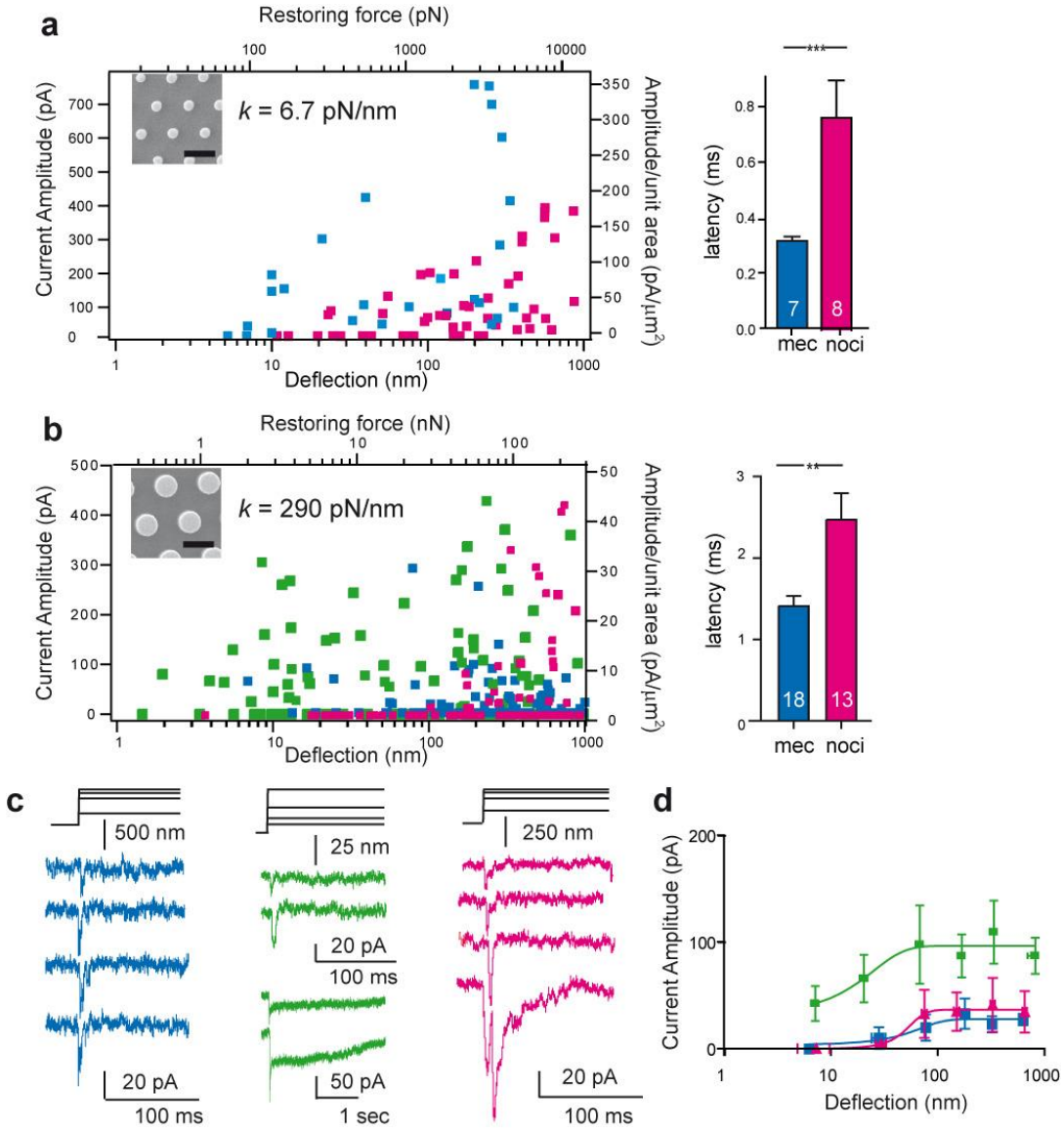

Supplementary Figure 3: Mechanosensitive properties of sensory neurons

(**a**) A stimulus-response plot of individual data points (blue-mechanoreceptors; magenta- nociceptors) collected on arrays where *k* = 6.7 pN/nm (insert scale bar 5 μm). In mechanoreceptors mechanically-gated currents are observed when pili are deflected as little as 10 nm, however, in nociceptors, larger deflections are required. Data represents 22 currents from 7 mechanoreceptors and 48 currents from 8 nociceptors. The latency of channel gating was significantly shorter in mechanoreceptors vs nociceptors (*n* is number of cells; Student's *t*-test, *** $p < 0.001$). (**b**) Stimulus-response plot of individual data points (blue-Type I mechanoreceptors; green- Type II mechanoreceptors; magenta- nociceptors) collected on arrays where *k* = 290 pN/nm (insert scale bar 5 μm). Channel gating in mechanoreceptors can occur with cell-substrate deflections of tens of nanometers, whereas much larger deflections are required for channel gating in nociceptors, (Type I mechanoreceptors: 114 measurements, 9 cells; Type II mechanoreceptors: 129 measurements, 8 cells; nociceptors: 110 data pts/13 cells). The latency of channel gating was, again, significantly shorter in mechanoreceptors vs nociceptors (*n* is number of cells; Student's *t*-test, * $p < 0.05$). The longer latencies on pili where *k* = 290 pN/nm likely reflect a dampening of the stimulus by the stiffer substrate. (data in (**b**) also shown in Figure 3). (**c**) Current traces from individual neurons; Type I mechanoreceptor (blue), Type II mechanoreceptor (green) and nociceptor (magenta). (**d**) Averaged stimulus-response curves for Type I (blue symbols/trace), Type II (green symbols/trace) mechanoreceptors and nociceptors (magenta symbols/trace). Data has been fit with a Boltzmann function with constraint that the minimum value is set to zero (Type I: 114 measurements from 9 cells; Type II: 129 measurements from 8 cells; Nociceptor: 110 data pts from 13 cells).

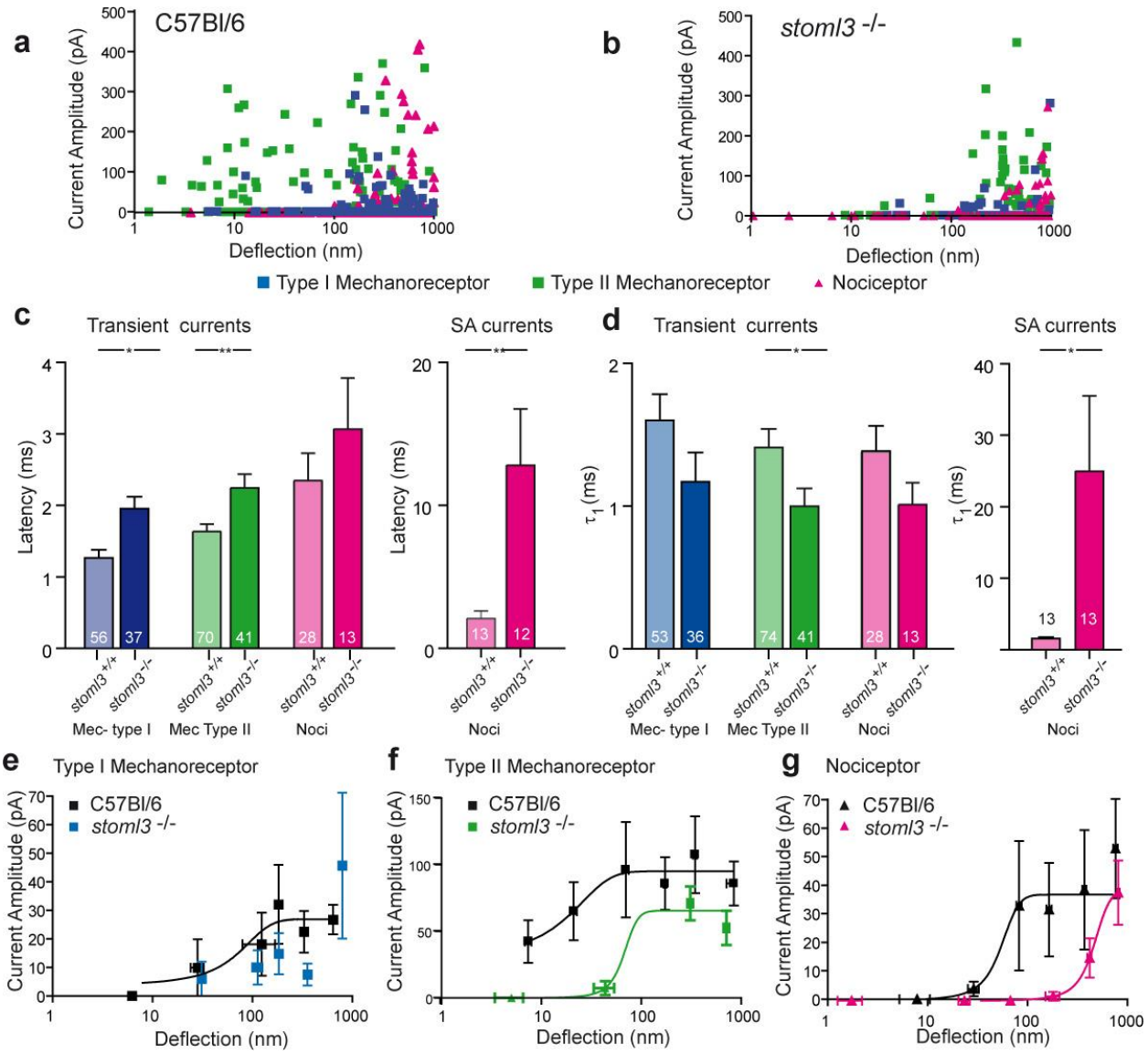

Supplementary Figure 4: Mechanosensitivity is reduced in sensory neurons from *stoml3*$^{-/-}$ mice

(**a**) Stimulus-response curves with all individual data points for sensory neurons isolated from C57Bl/6 mice (Type I mechanoreceptors: 114 measurements, 9 cells; Type II mechanoreceptors: 129 measurements, 8 cells; nociceptors: 110 measurements, 13 cells). (**b**) Stimulus-response curves with all individual data points for sensory neurons isolated from *stoml3*$^{-/-}$ mice (Type I mechanoreceptors: 48 measurements, 7 cells; Type II mechanoreceptors: 94 measurements, 8 cells; nociceptors: 89 measurements, 9 cells). (**c**) The latency of channel gating was significantly shorter for Type I mechanoreceptors; Type II mechanoreceptors and SA currents in nociceptors for neurons isolated from C57Bl/6 mice versus those isolated from the *stoml3*$^{-/-}$ mice (Student's *t*-test; * $p < 0.05$; ** $p < 0.01$). (**d**) There is a trend for a shorter time constant of activation (τ_1) of transient currents in all cell types isolated from the *stoml3*$^{-/-}$ mice; this was only significant for Type II mechanoreceptors (Student's *t*-test; * $p < 0.05$). In contrast, τ_1 for SA-currents in nociceptors isolated from *stoml3*$^{-/-}$ mice was significantly longer than observed for SA-currents in cells isolated from C57Bl/6 mice (Student's *t*-test, * $p < 0.05$). Data obtained for cells cultured on arrays with $k = 290$ pN/nm; *n* numbers indicated on graphs represent number of currents measured within each data set and used for this analysis, data displayed as mean ± s.e.m. (**e**) Stimulus response curves for wild-type Type I mechanoreceptors (black symbols/trace, data averaged from 114 measurements from 9 cells) vs *stoml3*$^{-/-}$ mice (blue symbols/trace, data averaged from 48 measurements from 7 cells). (**f**) Stimulus-response curves for wild-type, (black symbols/trace, 129 measurements, 8 cells) vs *stoml3*$^{-/-}$ Type II mechanoreceptors (green symbols/trace, 94 measurements, 8 cells). (**g**) Averaged stimulus-response curves for wild type (black symbols/trace, 110 measurements, 13 cells) vs *stoml3*$^{-/-}$ nociceptors (magenta symbols/trace, 89 measurements, 9 cells). (**e-g**) Data have been fit with a Boltzmann function with constraint that the minimum value is set to zero; points displayed as mean ± s.e.m. in both x and y.)

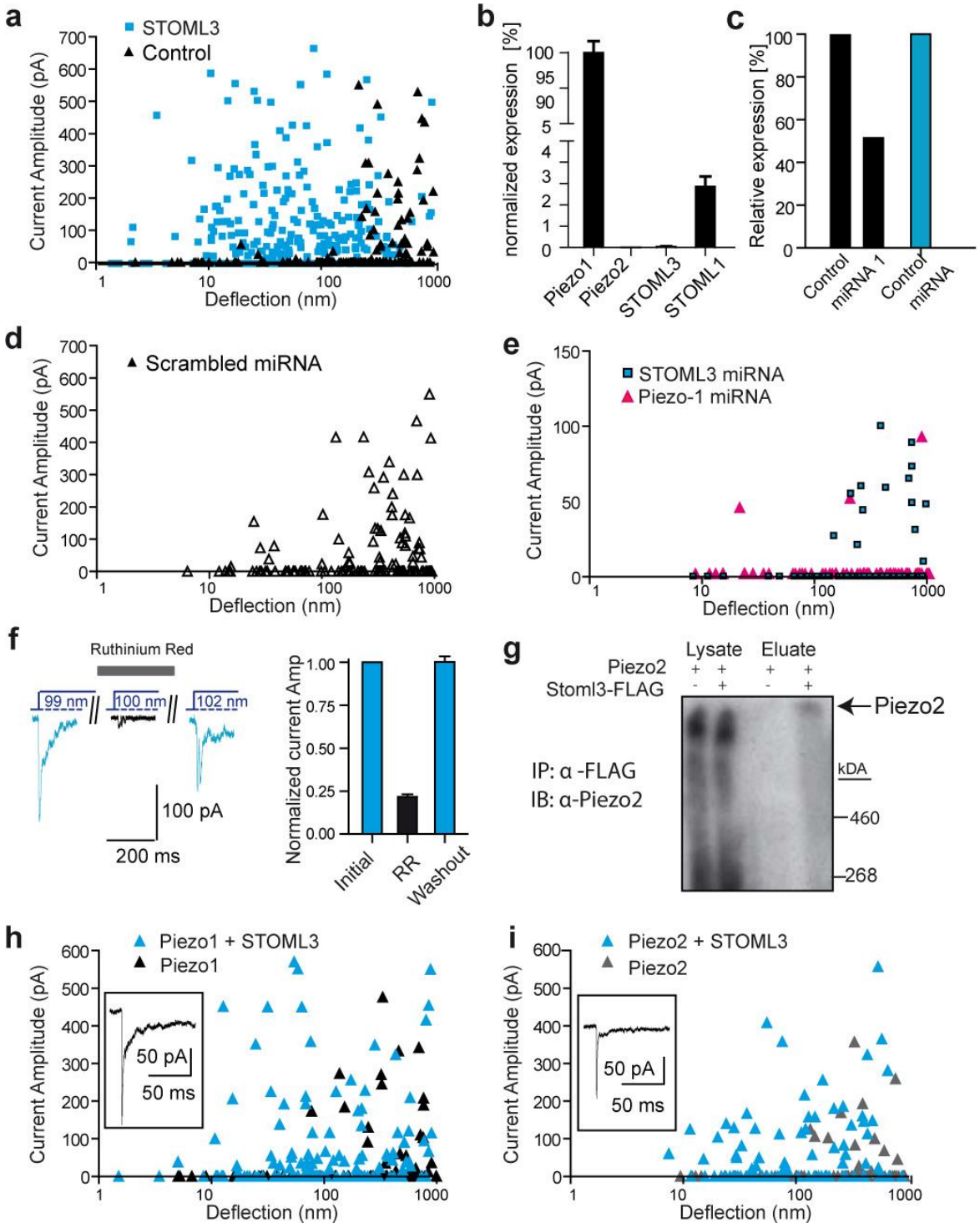

Supplementary Figure 5: STOML3 tunes Piezo channel-mediated mechanosensitivity

(a) Stimulus-response curves with all individual data points for N2a cells expressing Lifeact-mCherry (Control: 243 measurements, 19 cells) or STOML3-mGFP (297 measurements, 19 cells); (**b**) Normalized, endogenous transcript levels in control N2a cells (**c**) Transcript levels in N2a cells treated with miRNA: black, endogenous Piezo1± miRNA; cyan, overexpressed STOML3 ± miRNA. (**d-e**) Stimulus-response curves, all individual data points for N2a cells expressing (**d**) Piezo1 miRNA (100 measurements, 10 cells); (**e**) STOML3 miRNA2 (118 measurements, 10 cells); scrambled miRNA (145 measurements, 12 cells); (**f**) Application of Ruthenium Red to N2a cells overexpressing STOML3; representative current traces, current amplitude was normalized against pre-treatment currents, data represents average of triplicate measurements. (**g**) Western blot from STOML3-mediated pulldown of Piezo2, detected using an anti-Piezo2 antibody. (**h-i**) Stimulus-response curves with all individual data points for HEK-293 cells expressing (**h**) Piezo1 (103 measurements, 9 cells) or Piezo1 plus fluorescently-tagged STOML3 (135measurments, 11 cells); (**i**) Piezo2 (107 measurements, 10 cells) or Piezo2 plus fluorescently-tagged STOML3 (93 measurments, 9 cells). Inserts are representative currents.

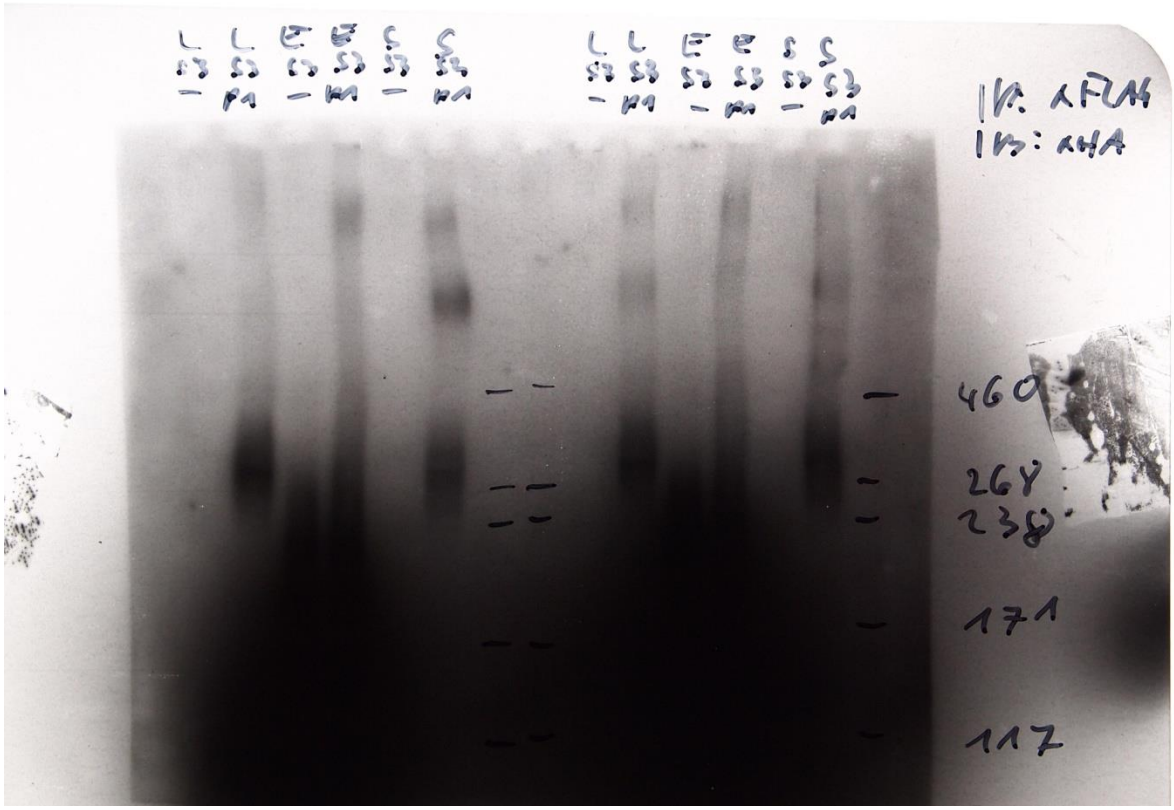

Supplementary Figure 6. Original blot presented in Figure 5g.

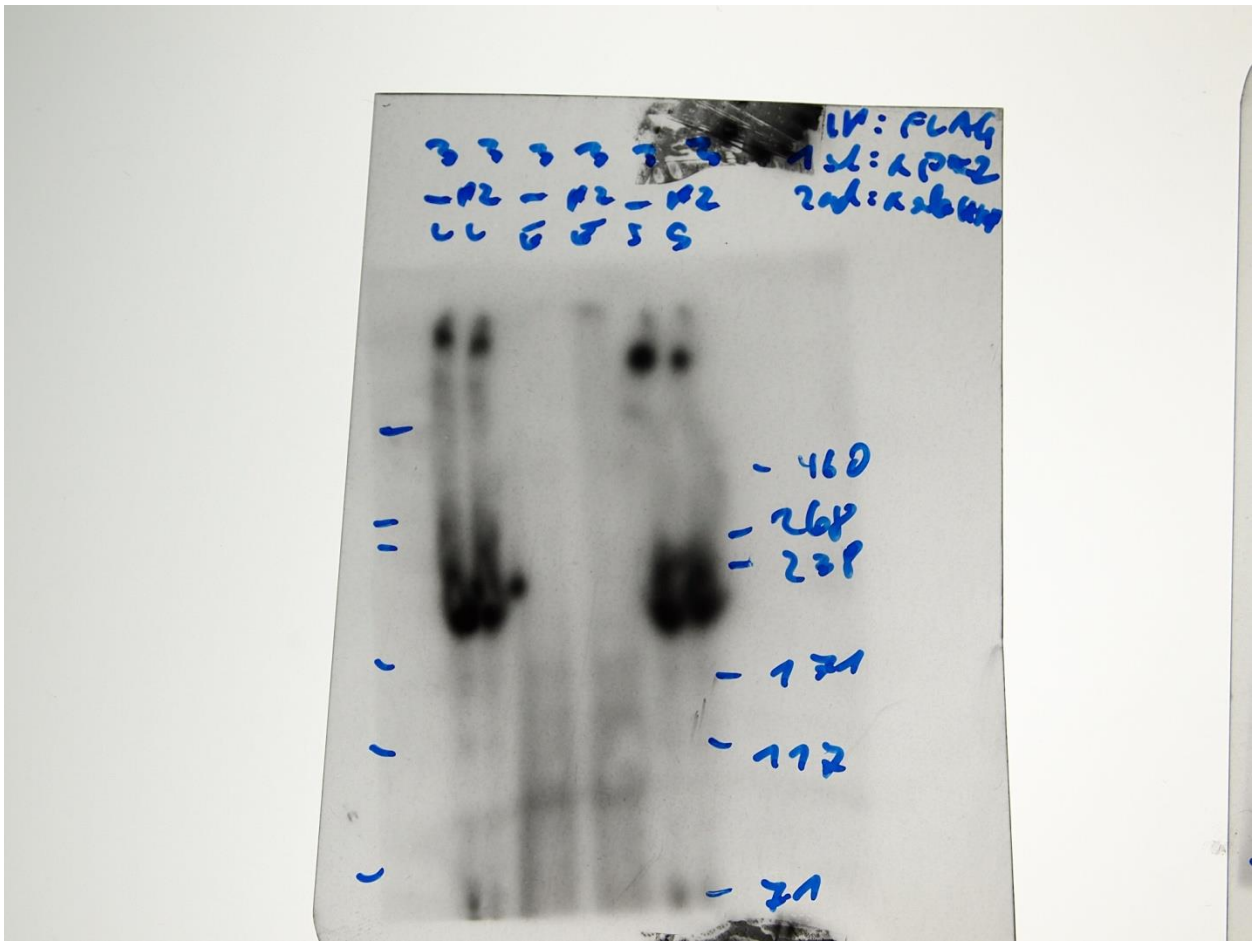

Supplementary Figure 7. Original blot presented in Supplementary Figure 5g.

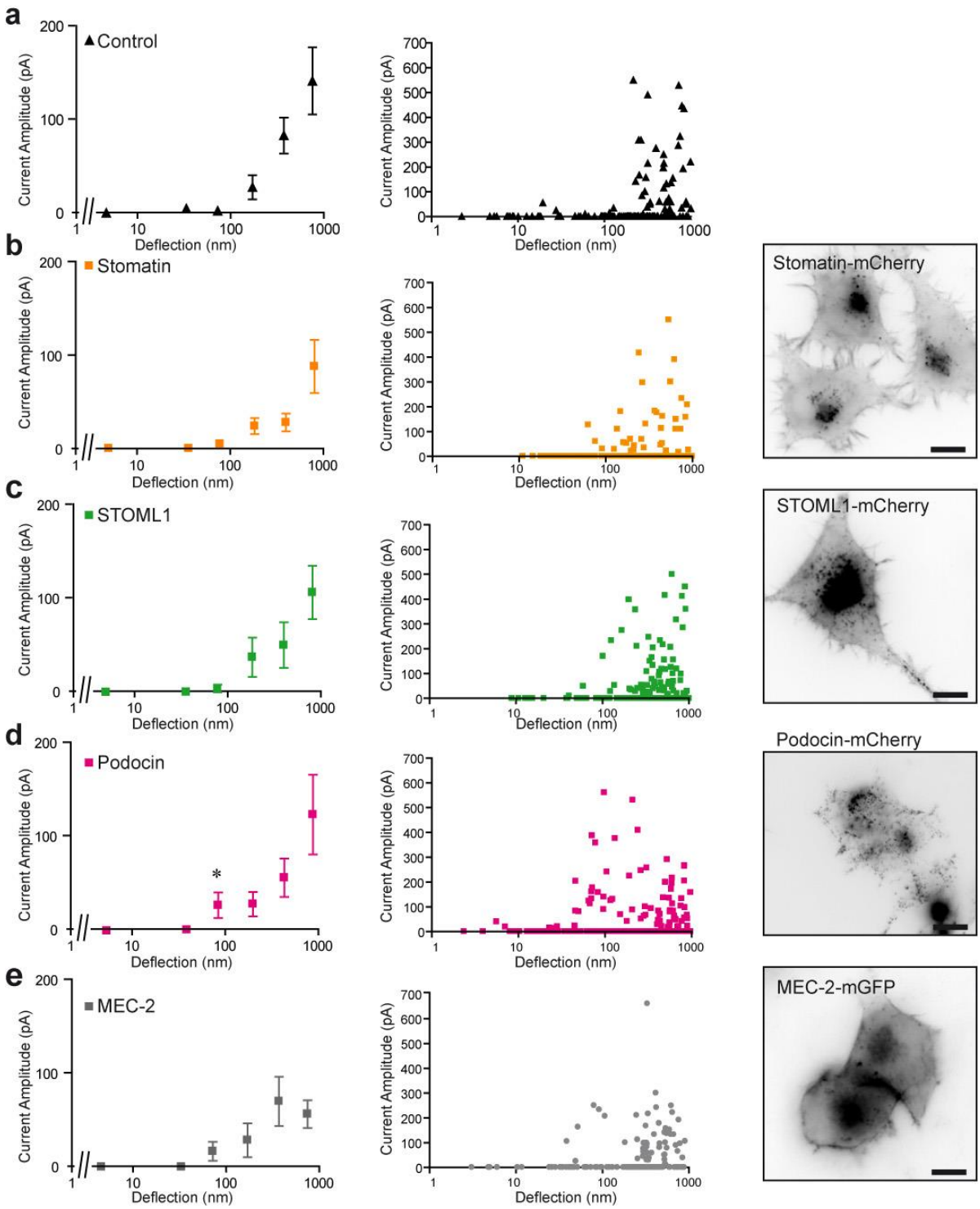

Supplementary Figure 8. Stomain-domain proteins and N2a cell mechanosensitivity

(**a**-**e**) Stimulus-response curves with all individual data points and the corresponding plots averaged across cells for N2a cells expressing fluorescently-tagged (**a**) Lifeact (243 measurements, 26 cells); (**b**) Stomatin (132 measurements, 15 cells); (**c**) STOML1 (176 measurements, 12 cells); (**d**) Podocin (237 measurements, 15 cells); (**e**) MEC-2 (149 measurements, 13 cells). Star indicates data point significantly different from control (**a**), (Students's *t*-test, * $p < 0.05$; data presented as mean ± s.e.m.). Inverted epi-fluorescent images are presented to show cellular distribution of over-expressed proteins, scale bar 10 μm. In all cases the over expressed stomatin-domain family protein is localized to the plasma membrane and an intracellular vesicle pool, as previously described for Stomatin and STOML3[40].

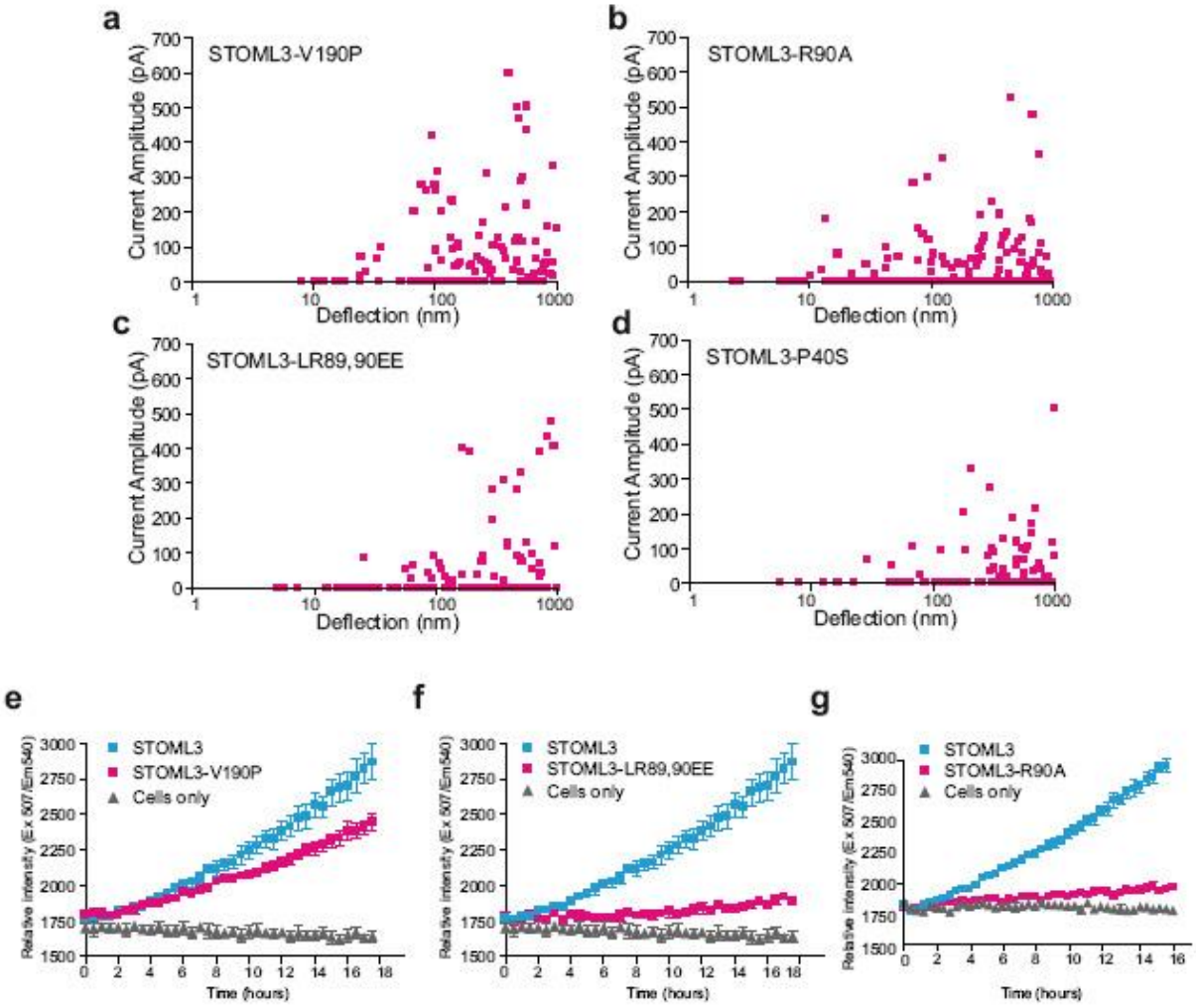

Supplementary Figure 9: The effect on mechanotransduction and oligomerization of STOML3 mutations

(**a-d**) Stimulus-response curves with all individual data points for N2a cells expressing (**a**) STOML3-V190P-mGFP (172 measurements, 15 cells); (**b**) STOML3-R90A-mGFP (218 measurements, 15 cells) (**c**) STOML3-LR89,90EE-mGFP (136 measurements, 12 cells).(**d**) STOML3-P40S-mGFP (142 measurements, 15 cells) (**e-g**) Signal development in BiFC assay of STOML3 oligomerization. Cells were transfected with a plasmid encoding STOML3 fused to the N-terminal BiFC fragment (VN) as bait. Fusion proteins of STOML3 variants containing mutations V190P (**e**), LR89,90EE (**f**) or P40S (**g**) with the C-terminal BiFC fragment (VC) were used as prey. As a positive control wtSTOML3-VC was used as prey. Data presented in each graph were compared from a single plate, represent an average of four transfections for each condition and are displayed as mean ± s.e.m.

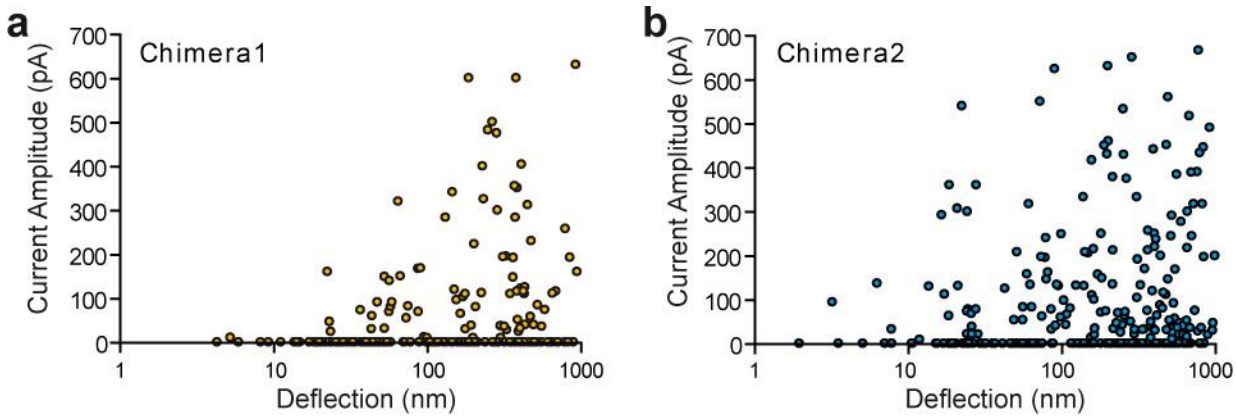

Supplementary Figure 10: Stimulus-response curves for N2a cells expressing STOML3-Stomatin chimeras

N2a cells expressing (**a**) Chimera1-mGFP (220 measurements, 15 cells) or, (**b**) Chimera2-mCherry (299 measurements, 14 cells). Note that when Chimera2 is present, mechanically-gated currents are observed with molecular-scale pillar deflections.

	C57Bl/6 Type I mec	C57Bl/6 Type II Mec	C57Bl/6 Noci
	Pillar array	Pillar array	Pillar array
Mice Cells Stimulation Pts Measurements	6 9 24 114	7 8 19 129	9 13 24 110
RA -latency (ms) - τ_1 (ms) - τ_2 (ms)	29 currents 1.2 ± 0.2 0.75 ± 0.2 2.6 ± 0.4	25 currents 1.2 ± 0.2 0.9 ± 0.2 3.0 ± 0.2	10 currents 1.8 ± 0.3 1.1 ± 0.3 2.8 ± 0.5
IA -latency (ms) - τ_1 (ms) - τ_2 (ms)	25 currents 1.2 ± 0.1 2.5 ± 0.2 19.4 ± 5.8	46 currents 1.7 ± 0.1 1.7 ± 0.1 39 ± 7.7	14 currents 2.6 ± 0.7 1.3 ± 0.2 48.7 ± 17
SA -latency (ms) - τ_1 (ms) - τ_2 (ms)	- 	- 	18 currents 2.6 ± 0.6 1.7 ± 0.2
	stoml3$^{-/-}$ Type I mec	*stoml3*$^{-/-}$ Type II Mec	*stoml3*$^{-/-}$ Noci
	Pillar array	Pillar array	Pillar array
Mice Cells Stimulation Pts Measurements	5 7 11 48	6 8 16 94	7 9 17 89
RA -latency (ms) - τ_1 (ms) - τ_2 (ms)	28 currents 1.7 ± 0.2 0.7 ± 0.1 1.2 ± 0.2	19 currents 2.5 ± 0.3 0.8 ± 0.2 2.4 ± 0.2	4 currents 7.8 ± 2.7 0.75 ± 0.2 2.6 ± 0.4
IA -latency (ms) - τ_1 (ms) - τ_2 (ms)	9 currents 2.2 ± 0.4 2.4 ± 0.6 19 ± 4.7	22 currents 2.0 ± 0.2 1.1 ± 0.1 35.9 ± 8.4	10 currents 2.5 ± 0.6 2.3 ± 0.8 58.1 ± 28
SA -latency (ms) - τ_1 (ms) - τ_2 (ms)	- 	- 	13 currents 13.5 ± 4.3 28.3 ± 11.7 -

Supplementary Table 1: **Physiological properties of recorded Type I mechanoreceptor, Type II mechanoreceptor and nociceptor neurons**

Neuronal cells were isolated from both C57Bl/6 and *stoml3*$^{-/-}$ mice. For each group the mechanical latency, activation time constant (τ_1 the time constant calculated from a mono-exponential fit of the current activation) and inactivation time constant (τ_2 the inactivation time constant calculated from a mono-exponential fit of the current inactivation, when relevant) are shown. Data are displayed as mean ± s.e.m.

	0-10	10-50	50-100	100-250	250-500	500-1000
Sensory neurons: C57Bl/6 mice						
Type I vs Type II mechanoreceptors	* (5,6)	** (7,5)	*(7,5)	NS (7,5)	NS (8,3)	NS (6,4)
Sensory neurons: C57Bl/6 mice vs *stoml3*$^{-/-}$ mice						
Type I mechanoreceptors Wild type vs *stoml3*$^{-/-}$	na	NS (7,6)	NS (7,6)	NS (7,6)	NS (8,6)	NS (6,6)
Type II mechanoreceptors Wild type vs *stoml3*$^{-/-}$	*(5,6)	*** (5,6)	** (5,5)	NS (4,6)	NS (4,6)	na
Nociceptors Wild type vs *stoml3*$^{-/-}$	NS (9,7)	NS (9,7)	NS (8,7)	* (7,8)	NS (9,6)	NS (9,8)

Supplementary Table 2: Statistical comparison of mechanically-gated current amplitude subsets of sensory neurons.

For each individual cell, currents were binned in the size ranges indicated and the currents within each bin averaged. Bins were subsequently averaged across cells and then a Student's *t*-test (after testing that data was normally distributed) was used to determine significance. NS indicates no significant difference between two samples, na indicates that there were either too few data points to make a comparison, or all of the measurements within a bin were equal to zero. In all cases * indicates $p < 0.05$; ** indicates $p < 0.01$; *** indicates $p < 0.001$. *n* numbers in brackets indicate the number of data points within each bin that were statistically compared.

	Control	STOML3	Stomatin	STOML1	Podocin	MEC-2
Transfections	7	10	4	5	4	4
Cells	31	19	15	12	15	13
Stimulation Pts	58	35	24	21	33	22
Measurements	388	297	132	176	237	149
RA-like	34%	34%	24%	24%	30%	32%
-latency (ms)	2.6 ± 0.4	1.9 ± 0.2	2.9 ± 0.9	1.6 ± 0.3	3.1 ± 0.9	2.2 ± 0.6
- τ_1 (ms)	0.8 ± 0.2	0.8 ± 0.1	0.8 ± 0.3	0.8 ± 0.1	1.0 ± 0.2	0.7 ± 0.2
- τ_2 (ms)	2.1 ± 0.2	1.6 ± 0.2	1.4 ± 0.3	1.4 ± 0.2	1.4 ± 0.2	1.9 ± 0.3
IA-like	31%	36%	24%	26%	25%	40%
-latency (ms)	3.0 ± 0.5	2.3 ± 0.4	2.3 ± 0.7	1.5 ± 0.2	4.1 ± 1.1	2.5 ± 0.4
- τ_1 (ms)	1.1 ± 0.3	2.2 ± 0.4	1.0 ± 0.2	1.9 ± 0.5	2.8 ± 0.1	1.5 ± 0.2
- τ_2 (ms)	23.0 ± 2.4	18.6 ± 1.4	16.2 ± 2.5	16.8 ± 3.0	18.0 ± 3.2	18.0 ± 2.8
SA-like	35%	30%	51%	50%	44%	27%
-latency (ms)	2.3 ± 0.5	1.9 ± 0.2	1.9 ± 0.4	2.3 ± 0.4	2.9 ± 0.4	1.8 ± 0.4
- τ_1 (ms)	2.1 ± 0.4	2.5 ± 0.3	1.7 ± 0.3	3.6 ± 0.8	1.0 ± 0.2	2.5 ± 0.7
- τ_2 (ms)	-	-	-	-	-	-
	STOML3-V190P	**STOML3-R90A**	**STOML3-LR89,90EE**	**STOML3-P40S**	**Chimera1**	**Chimera2**
Transfections	6	4	6	4	4	4
Cells	15	15	12	15	15	14
Stimulation Pts	30	29	20	29	28	24
Measurements	172	218	136	142	220	299
RA-like	39%	31%	25%	36%	57%	43%
-latency (ms)	1.9 ± 0.3	1.7 ± 0.4	2.5 ± 0.5	1.9 ± 0.3	2.4 ± 0.4	3.0 ± 0.3
- τ_1 (ms)	0.8 ± 0.2	0.8 ± 0.2	0.6 ± 0.1	0.8 ± 0.2	0.8 ± 0.2	0.6 ± 0.8
- τ_2 (ms)	1.7 ± 0.2	2.1 ± 0.2	1.9 ± 0.3	1.3 ± 0.2	1.5 ± 0.2	1.6 ± 0.2
IA-like	32%	35%	40%	35%	19%	22%
-latency (ms)	1.7 ± 0.2	2.2 ± 0.4	2.8 ± 0.4	1.9 ± 0.3	3.8 ± 1.1	3.1 ± 0.5
- τ_1 (ms)	1.2 ± 0.2	1.7 ± 0.4	1.1 ± 0.3	0.9 ± 0.3	1.1 ± 0.4	0.8 ± 0.2
- τ_2 (ms)	16 ± 2.2	18 ± 2.3	14.5 ± 2.3	16 ± 2.5	16 ± 3.0	15 ± 2.2
SA-like	28%	33%	34%	28%	23%	35%
-latency (ms)	1.9 ± 0.3	1.9 ± 0.3	2.2 ± 0.3	3.1 ± 0.8	2.6 ± 0.5	2.5 ± 0.3
- τ_1 (ms)	1.7 ± 0.3	2.3 ± 1	1.4 ± 0.2	1.3 ± 0.7	1.2 ± 0.73	1.5 ± 0.2
- τ_2 (ms)	-	-	-	-	-	-

Supplementary Table 3: **Electrophysiological properties of N2a cells overexpressing stomatin-domain family proteins or variants of STOML3.** For each group, currents were classed as RA-like (τ_2 < 5 ms), IA- like (τ_2 5-50 ms) or SA-like (τ_2 > 50 ms). The fraction of currents classed in each group, the mechanical latency, activation time constant ($\tau_{1;}$ calculated from a mono-exponential fit of the current activation) and inactivation time constant (τ_2; calculated from a mono-exponential fit of the current inactivation, when relevant) are shown as mean ± s.e.m. Control cells were transfected with a plasmid encoding LifeAct alone and in this case includes data collected for cells expressing the scrambled miRNA.

	0-10	10-50	50-100	100-250	250-500	500-1000
N2a Cells						
STOML3 vs control	na	*** (17,26)	*** (15,25)	*** (12,26)	NS (7,25)	na
N2a Cells: miRNA knockdowns						
Scram vs Piezo1 miRNA	na	na	na	NS (9,10)†	** (9,10)†	*** (9,10)†
Scram vs STOML3 miRNA	na	na	na	NS (11,10)†	** (11,10)†	** (9,10)†
N2a Cells: STOML3 variants						
V190P vs control	na	NS (15,26)	NS (13,25)	NS (15,26)	NS (14,25)	NS (11,21)
V190P vs STOML3	na	*** (15,17)	** (13,16)	* (15,12)	NS (14,7)	na
R90A vs control	na	NS (12,26)	NS (10,25)	NS (12,26)	NS (11,25)	NS (7,21)
R90A vs STOML3	NS (12,12)	*** (12,17)	* (10,16)	** (12,12)	NS (11,7)	na
LR89.90EE vs control	na	NS (13,26)	NS (12,25)	NS (13,26)	NS (12,25)	NS (10,21)
LR89.90EE vs STOML3	na	***(13,17)	** (12,16)	*** (13,12)	NS (12,7)	na
P40S vs control	na	NS (15,26)	NS (15,25)	NS (14,26)	* (13,25)	NS (15,21)
P40S vs STOML3	na	*** (15,17)	*** (15,16)	*** (14,12)	*** (13,7)	na
Chimera1 vs Chimera2	NS (13,5)	* (12,11)	NS (11,7)	* (14, 11)	NS (13,13)	NS (12,11)
Chimera1 vs control	na	NS (12,26)	** (11,25)	NS (14, 26)	NS (13,25)	NS (12,21)
Chimera1 vs STOML3	NS (13,12)	*** (12,17)	* (11,16)	** (14, 12)	NS (13,7)	na
Chimera2 vs control	na	*** (11,26)	*** (7,25)	*** (11,26)	NS (13,25)	NS (11,21)
Chimera2 vs STOML3	NS (5,12)	**NS** (11,17)	**NS** (7,16)	**NS** (11,12)	NS (13,7)	na
N2a Cells : Stomatin domain proteins						
STOM vs control	na	na	NS (15,25)	NS (15,26)	NS (15,25)	NS (15, 21)
STOM vs STOML3	na	na	** (15,16)	*** (15,12)	*** (15,7)	na
STOML1 vs control	na	NS (12, 26)	NS (12,25)	NS (12,26)	NS (12,25)	NS (11,21)
STOML1 vs STOML3	NS	*** (12,17)	** (12,16)	*** (12,12)	* (12,7)	na
Podocin vs control	na	NS (15,26)	* (14,25)	NS (14,26)	NS (14,25)	NS (14, 21)
Podocin vs STOML3	NS (15,12)	*** (15,17)	** (14,16)	*** (14,12)	* (14,7)	na
MEC-2 vs control	na	na	NS (13,25)	NS (13,26)	NS (12,25)	NS (10,21)
MEC-2 vs STOML3	na	na	** (13,16)	** (13,12)	NS (12,7)	na
HEK-293 cells						
Piezo1 vs Piezo1 + STOML3	na	** (9,8)	* (9,10)	** (9,10)	NS (9,6)	NS (7,6)
Piezo2 vs Piezo2 + STOML3	na	* (9,8)	* (9,7)	* (9,7)	* (9,7)	** (8,4)

Supplementary Table 4. Statistical comparison of mechanically-gated current amplitude in the presence of Stomatin-like proteins and variants. For each individual cell, currents were binned in the size ranges indicated and the currents within each bin averaged. Bins were subsequently averaged across cells and then a Student's *t*-test (when data normally distributed) or Mann Whitney† test (for non-parametric data sets) was used to compare bins between samples. All stomatin-like proteins and STOML3 variants were compared with results from cells overexpressing STOML3 or control N2a cells. NS indicates no significant difference between two samples, na indicates that there were either too few data points to make a comparison, or all of the measurements within a bin were equal to zero. In all cases * $p < 0.05$; ** $p < 0.01$; *** $p < 0.001$. *n* numbers in brackets indicate data points (i.e. cells) within each bin that were statistically compared. STOML3 significantly increased mechanotransduction with deflections of 10-50, 50-100 and 100-250 nm in comparison with control N2a cells; as did Chimera2. N2a mechanosensitivity of cells overexpressing Chimera2 was not significantly different in comparison with cells overexpressing STOML3, indicating that the STOML3-stomatin domain is necessary for the increase in N2a mechanosensitivity. The only other proteins that differed significantly from the control within any of the stimulus ranges were Chimera1 (50-100 nm) and Podocin (50-100nm); however in both cases the cellular response was still significantly smaller than in the presence of STOML3.This indicates that Chimera1 and Podocin can marginally shift the mechanosensitivity range in N2a cells.

	HEK-293 Piezo1	HEK-293 Piezo1 + STOML3	HEK-293 Piezo2	HEK-293 Piezo2 + STOML3
Transfections	4	5	4	5
Cells	9	11	10	9
Stimulation Pts	17	18	19	16
Measurements	103	135	107	93
RA-like	10%	37%	23%	53%
-latency (ms)	1.0 ± 0.	2.2 ± 0.4	2.4 ± 0.6	2.3 ± 0.4
- τ_1 (ms)	0.6 ± 0.2	0.5 ± 0.1	0.5 ± 0.1	0.7 ± 0.1
- τ_2 (ms)	2.3 ± 0.4	1.5 ± 0.3	1.2 ± 0.4	1.5 ± 0.2
IA-like	41%	35%	23%	27%
-latency (ms)	1.4 ± 0.2	2.2 ± 0.5	4.3 ± 1.2	1.5 ± 0.4
- τ_1 (ms)	0.9 ± 0.2	1.0 ± 0.1	2.4 ± 0.6	0.8 ± 0.1
- τ_2 (ms)	16 ± 2.2	20 ± 2.8	29 ± 10	20 ± 4.7
SA-like	48%	28%	54%	20%
-latency (ms)	2.4 ± 0.7	2.1 ± 0.4	2.0 ± 0.32	2.6 ± 0.6
- τ_1 (ms)	2.0 ± 0.7	2.0 ± 0.3	4.4 ± 1.2	1.1 ± 0.3
- τ_2 (ms)	-	-	-	-

Supplementary Table 5: **Electrophysiological properties of HEK-293 cells overexpressing Piezo1 or Piezo2 in the presence and absence of STOML3.** For each group currents were classed as RA-like (τ_2 < 5 ms), IA- like (τ_2 5-50 ms) or SA-like (τ_2 > 50 ms). The fraction of currents classed in each group, the mechanical latency, activation time constant (τ_1) and inactivation time constant (τ_2) are shown as mean ± s.e.m.

Construct Name	Plasmid used	Encodes	Source	Thanks to
mStoml3-mEGFP	pEGFP-N3 (Clontech)	STOML3-mEGFP	Current study	
mStoml3-mCherry	pEGFP-N3 (Clontech)	STOML3-mCherry	Lapatsina et al 2012[1]	
lifeact-mCherry	pEGFP-N3 (Clontech)	MGVADLIKKFESISKEE-mCherry	Current study	
lifeact-mEGFP	pEGFP-N3 (Clontech)	MGVADLIKKFESISKEE-mGFP	Current study	
Chimera 1	pEGFP-N3 (Clontech)	m STOML3$^{1-86}$[Stom$^{94-202}$] STOML3$^{196-282}$ mEGFP	Current study	
Chimera 2	pEGFP-N3 (Clontech)	mStom$^{1-93}$[S STOML3$^{87-195}$] Stom$^{203-284}$ mCherry	Current study	
Stom-mCherry	pEGFP-N3 (Clontech)	Stomatin-mCherry	Brand et al 2012[2]	
Mec2-mEGFP	pEGFP-N3 (Clontech)	MEC-2-mEGFP	Current study	Miriam Goodman for MEC-2 cDNA
mStoml1-mCherry	pEGFP-N3 (Clontech)	STOML1-mCherry	Current study	Alexei Kozlenkov
mPodocin-mCherry	pEGFP-N3 (Clontech)	Podocin-mCherry	Current study	Eric Honoré for podocin cDNA
mStoml3-P40S-EGFP	pEGFP-N3 (Clontech)	STOML3-P40S-EGFP	Lapatsina et al 2012[1]	
mStoml3-R90A-mEGFP	pEGFP-N3 (Clontech)	STOML3-R90A-mEGFP	Current study	
mStoml3-LR89,90EE-mEGFP	pEGFP-N3 (Clontech)	STOML3-LR89,90EE-mEGFP	Current study	
mStoml3-V190P-mEGFP	pEGFP-N3 (Clontech)	STOML3-V190P-mEGFP	Current study	
mStoml3-VC	pBiFC-VC155	STOML3-VC	Current study	Chang-Deng Hu for pBiFC-VC155 Alexei Kozlenkov
mStoml3-VN	pBiFC-VN173	STOML3-VN	Current study	Chang-Deng Hu for pBiFC-VC173 Alexei Kozlenkov
mStoml3-V190P-vc	pBiFC-VC155	STOML3-V190P-VC	Current study	
mStoml3-R90A-vc	pBiFC-VC155	STOML3-R90A-VC	Current study	
mStoml3-LR89,90EE-vc	pBiFC-VC155	STOML3-LR89,90EE-VC	Current study	
	pcDNA 3.1(-) (Invitrogen)	Piezo1	Coste et al 2010[3]	Ardem Patapoutian
	pCMV-sport6 (Invitrogen)	Piezo2	Coste et al 2010[3]	Ardem Patapoutian
Fam38a-HA	pcDNA 3.1(-) (Invitrogen)	HA-Piezo1	Current study	Ardem Patapoutian for Piezo-1 cDNA

Supplementary Table 6: Plasmids used in this study

Target	Top strand	Bottom strand
Piezo1	5'-TGCTGTAAAGATGTCCTTCAGGTCCAGTTTTGG CCACTGACTGACTGGACCTGGGACATCTTTA-3'	5'-CCTGTAAAGATGTCCCAGGTCCAGTCAGTCAGT GGCCAAAACTGGACCTGAAGGACATCTTTAC-3'
STOML3	5'-TGCTGATGATCTTCAAGCACATCCATGTTTTGGC CACTGACTGACATGGATGTTTGAAGATCAT-3'	5'-CCTGATGATCTTCAAACATCCATGTCAGTCAGTG GCCAAAACATGGATGTGCTTGAAGATCATC-3’

Supplementary Table 7: Sequence of miRNAs used in this study

Supplementary References

1. Lapatsina, L. *et al.* Regulation of ASIC channels by a stomatin/STOML3 complex located in a mobile vesicle pool in sensory neurons. *Open Biol.* doi:10.1098/rsob.120096
2. Brand, J. *et al.* A stomatin dimer modulates the activity of acid-sensing ion channels. *EMBO J.* **31,** 3635–3646 (2012).
3. Coste, B. *et al.* Piezo1 and Piezo2 Are Essential Components of Distinct Mechanically Activated Cation Channels. *Science* **330,** 55–60 (2010).